

High- p_T π^0 Production with Respect to the Reaction Plane Using the PHENIX Detector at RHIC

David L. Winter^a for the PHENIX Collaboration

Columbia University, NY, NY 10027, USA

Received: date / Revised version: date

Abstract. The origin of the azimuthal anisotropy in particle yields at high p_T ($p_T > 5$ GeV/c) in RHIC collisions remains an intriguing puzzle. Traditional flow and parton energy loss models have failed to completely explain the large v_2 observed at high p_T . Measurement of this parameter at high p_T will help to gain an understanding of the interplay between flow, recombination and energy loss, and the role they play in the transition from soft to hard physics. Neutral mesons measured in the PHENIX experiment provide an ideal observable for such studies. We present recent measurements of π^0 yields with respect to the reaction plane, and discuss the impact current models have on our understanding of these mechanisms.

PACS. 25.75.-q , 25.75.Dw

1 Introduction

Two of the greatest mysteries that have arisen from the RHIC physics program are the source of the apparent flatness of the high p_T (> 5 GeV/c) suppression of R_{AA} [1] and the source of non-zero v_2 at high p_T [2]. The existence of intermediate to high p_T v_2 was suggested early in the RHIC program [3], and has been the subject of many theoretical treatments (see [4,5] for some additional examples). Traditional flow and parton energy loss pictures have failed to describe the magnitude of this anisotropy. Measurement of the azimuthal asymmetry v_2 at high p_T will shed light on the contributions from flow, recombination, and energy loss, as well as the transition from soft to hard production mechanisms.

2 Measuring v_2 and π^0 yields in PHENIX

The orientation of the reaction plane is measured event-by-event using the set of two PHENIX Beam-Beam Counters (BBCs), which reside at the region $3 < |\eta| < 4$. Each detector is an array of 64 hexagonal, close-packed quartz Cherenkov counters, located 150 cm from the interaction point. The charge measured by each counter is proportional (on average) to the multiplicity of particles hitting it. The reaction plane angle Ψ_{RP} is determined from the value of $\langle \cos 2\phi \rangle$. Because the two BBCs provide independent measurements of Ψ_{RP} , we can estimate the resolution of the combined measurement via standard techniques [6].

For measuring photons and π^0 s, we use the Electromagnetic Calorimeter (EMCal) [7]. Candidate clusters are

required to pass γ identification cuts, and m_{inv} distributions are formed from pairs of these clusters. The resulting yields are binned in angle with respect to the reaction plane ($\Delta\phi = \phi - \Psi_{RP}$). A similarly binned mixed event background is then subtracted. The counts in the remaining peak centered on the π mass are integrated in a $\pm 2\sigma$ window (where σ is the width of a Gaussian fit to the peak). Six bins in $\Delta\phi$ are used in the interval $[0 - \pi/2]$.

To measure v_2 , we fit the raw (uncorrected) $\Delta\phi$ distribution $Y(\Delta\phi)$ as

$$Y_{raw}(\Delta\phi) \propto 1 + 2v_2^{raw} \cos(2\Delta\phi). \quad (1)$$

The resulting v_2 parameter needs to be corrected for the reaction plane measurement resolution, hence the designation v_2^{raw} . The resolution σ_{RP} is determined for each centrality bin, and leads to the corrected value $v_2^{corr} = v_2^{raw}/\sigma_{RP}$. The yields as a function of $\Delta\phi$ can then be corrected with a factor

$$Y(\Delta\phi) = Y_{raw}(\Delta\phi) \times \frac{1 + 2v_2^{corr} \cos 2\Delta\phi}{1 + 2v_2^{raw} \cos 2\Delta\phi}. \quad (2)$$

3 Results and Discussion

To obtain $R_{AA}(\Delta\phi)$, we exploit the fact that the ratio of the yield at a given $\Delta\phi$ to the inclusive yield is equivalent to the ratio of the angle-dependent R_{AA} to the inclusive R_{AA} . Thus multiplying these relative yields by an inclusive measured R_{AA} , we have:

$$R_{AA}(\Delta\phi) = Y(\Delta\phi)/Y \times R_{AA} \quad (3)$$

The $R_{AA}(\Delta\phi, p_T)$ as a function of $\langle N_{part} \rangle$ is shown in Figure 1. We note that there appears to be a slightly

^a email: winter@nevis.columbia.edu

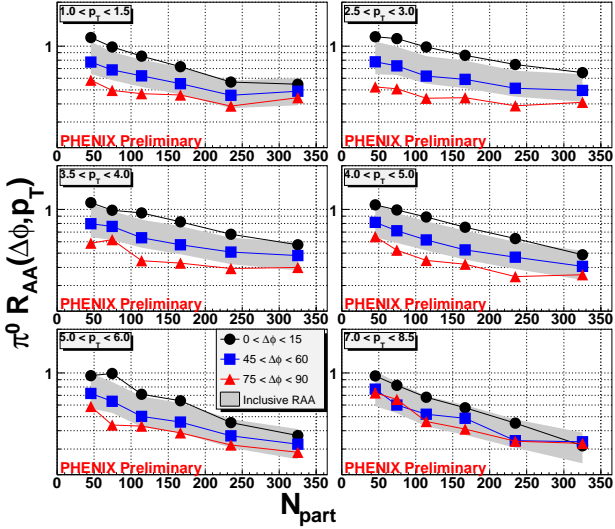


Fig. 1. $R_{AA}(p_T)$ as a function of $\langle N_{part} \rangle$ for Au+Au 200 GeV/c collisions; Each curve corresponds to a different $\Delta\phi$ bin and the panels are for different p_T bins. The grey bands indicate the systematic error due to the reaction plane resolution correction.

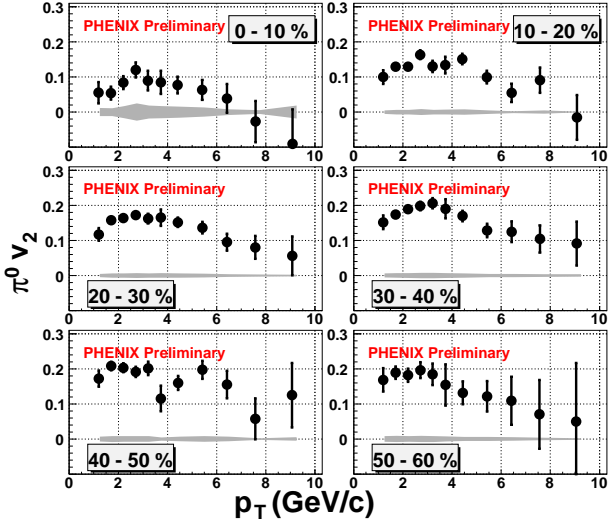


Fig. 2. $\pi^0 v_2(p_T)$ for Au+Au 200 GeV/c collisions, with each panel corresponding to a centrality bin. The grey bands indicate the systematic error due to the reaction plane resolution correction.

different centrality dependence, according which $\Delta\phi$ bin in which the R_{AA} is being measured. This feature is emphasized by plotting the data on a semi-log scale, showing that the R_{AA} behaves differently in different $\Delta\phi$ bins.

The resulting $\pi^0 v_2$ is shown in Figure 2. For the first time we observe v_2 up to 10 GeV/c. While the value of the v_2 decreases beyond intermediate p_T , it nonetheless shows a substantial and perhaps constant value out to the highest measured transverse momenta.

To gain insight into the v_2 mechanisms at work at high p_T , we turn to models. We compare the $\pi^0 v_2$ to

two models, a calculation done by Turbide et al. [8] (using an Arnold-Moore-Yaffe (AMY) formalism [9]) and the Molnar Parton Cascade (MPC) model [10]. Figure 3 shows calculations from these models, plotted alongside data for similar centralities. The AMY calculation contains energy loss mechanisms only, and we see that the data appear to decrease to a value at high p_T that is consistent with this model; the level of agreement is most striking in the 20-40% bin.

The MPC model has a number of mechanisms, including corona effects, energy loss, and the ability to boost lower p_T partons to higher p_T (a unique feature). The calculation shown in Figure 3 does a better job of reproducing the overall shape of the v_2 , though it is systematically low. It is important to note that this calculation is done for one set of parameters, so it should be very interesting to see if the MPC can better reproduce the data for a different set of parameters (the opacity of the medium, for example).

The prevailing thought is that the high p_T behavior of the v_2 is due to energy loss mechanisms. If this is true, the R_{AA} should be sensitive to the geometry of the collision. To test this behavior, we seek to combine the two traditional geometric parameters (centrality, or collision overlap, and angle of emission) into a single parameter, a quantity which we will refer to as “ $\rho L dL$ ”. Details of the calculation are described in [11], as well as below.

The Guylassy-Levai-Vitev (GLV) formalism can be used to calculate jet energy loss for a set of scattering centers $\{x_i\}$, where $x_i = (t_i, r_i)$. In practice, an average over these centers is performed. As shown in Figure 4, if a static uniform color charge density within some region ($\rho(x) = \rho_0$ and zero outside the region) is assumed, the resulting energy loss is $\Delta E_{QCD} \propto \rho_0 L_{max}^2$. More realistically, if the density seen by the particle changes along the path, we have $\Delta E_{QCD} \propto \int_0^L \rho(L) L dL$ (which reduces to the quadratic L dependence for a constant density). Application of this to a 1D Bjorken expansion, with

$$\rho(\mathbf{r}, \tau) = \rho(\mathbf{r}, \tau_0) \frac{\tau_0}{\tau} \quad (4)$$

and given a jet trajectory $\mathbf{r}(\tau) = \mathbf{r}_0 + \mathbf{v}(\tau - \tau_0)$ (assuming $v \simeq c = 1$ for the jet), we have

$$L(\tau) = |\mathbf{r}(\tau) - \mathbf{r}_0| = \tau - \tau_0 \quad (5)$$

Therefore we have

$$\Delta E_{QCD} \propto \int_0^{L_{max}} \rho(\mathbf{r}, \tau) L dL \quad (6)$$

$$\int_0^{L_{max}} \frac{\rho(\mathbf{r}, \tau_0) \tau_0 L}{\tau_0 + L} dL \quad (7)$$

This effective energy loss is calculated from the parton-density weighted average of the length from hard-scattering origin to edge of an ellipse. Additionally, we perform a Glauber Monte Carlo sampling of starting points to account for fluctuations in the location of the hard-scattering origin of the particles’ paths within the region of overlap between the colliding nuclei. The crucial feature of $\rho L dL$

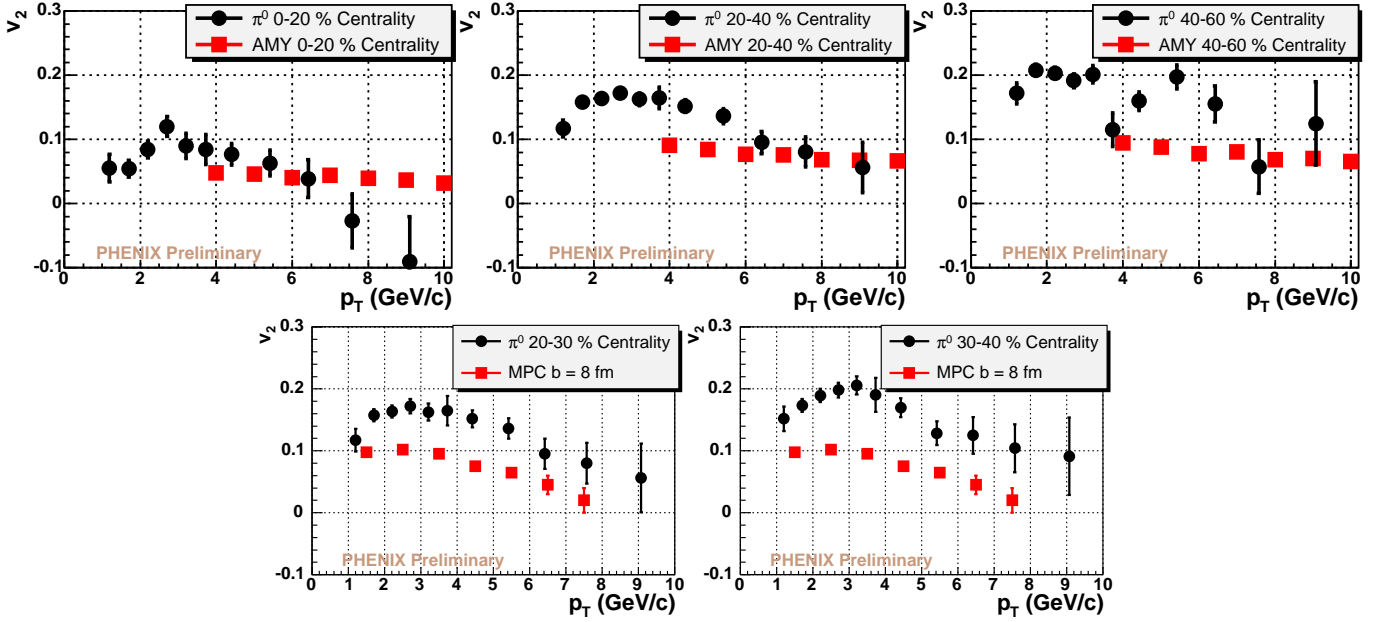


Fig. 3. Comparison of π^0 v_2 with models. The top three panels show the AMY calculation with data for three centralities [8]. The bottom two panels compare two centralities with the $b = 8$ fm calculation of the MPC model [10].

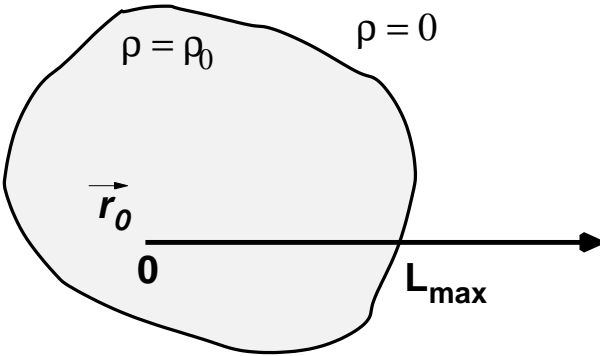


Fig. 4. Schematic of the calculation of $\int \rho L dL$. See text for details.

is that it is proportional to the energy loss sustained by the parton as it traverses the medium.

The resulting dependence of R_{AA} for all centralities and angles on $\rho L dL$ is shown in Figure 5. If the observed R_{AA} arose from only geometric effects, we would expect the data to exhibit a universal dependence on $\rho L dL$. For low p_T , this is clearly not the case; something more than just energy loss is taking place there. However, when the p_T reaches 7 GeV/c and above, the R_{AA} data do indeed appear to have a dependence on a single $\rho L dL$ curve. This apparent scaling strongly suggests that the dominant effect on R_{AA} at high- p_T is energy loss. These data can help to constrain energy loss models, and perhaps help to understand the nature of that energy loss (is it radiative, collisional, or some combination of both?).

4 Conclusions

We have presented the first measurement of high p_T v_2 for π^0 s. It is now clear that the v_2 at high p_T does decrease but to a non-zero value. Comparison of v_2 with models suggest that the dominant mechanism at work at high p_T is energy loss. In addition, we have presented the first measurement of π^0 R_{AA} as a function of angle with respect to the reaction plane. When the R_{AA} data are examined as a function of an effective path length through the medium, the scaling that arises at high p_T also argues for energy loss as the dominant mechanism at work.

References

1. T. Isobe, nucl-ex/0510085
2. S. Adler et al., *Phys. Rev. Lett.* **96**, 032302 (2006)
3. M. Guylassy et al., *Phys. Rev. Lett.* **86**, 2537 (2001)
4. E. Shuryak, *Phys. Rev.* **C66** 027902 (2002)
5. A. Drees et al., *Phys. Rev.* **C71** 034909 (2005)
6. A. M. Poskanzer, S. A. Voloshin, *Phys. Rev.* **C58**, 1671 (1998)
7. L. Aphecetche et al., *Nucl. Instr. Meth.* **A499** 521 (2003)
8. S. Turbide et al., *Phys. Rev.* **C72** 014906 (2005)
9. P. Arnold et al., *J. High Energy Phys.* **05**, 051 (2003)
10. D. Molnar, nucl-th/0503051
11. B. Cole, *Eur.Phys.J.* **C43**, 271 (2005)

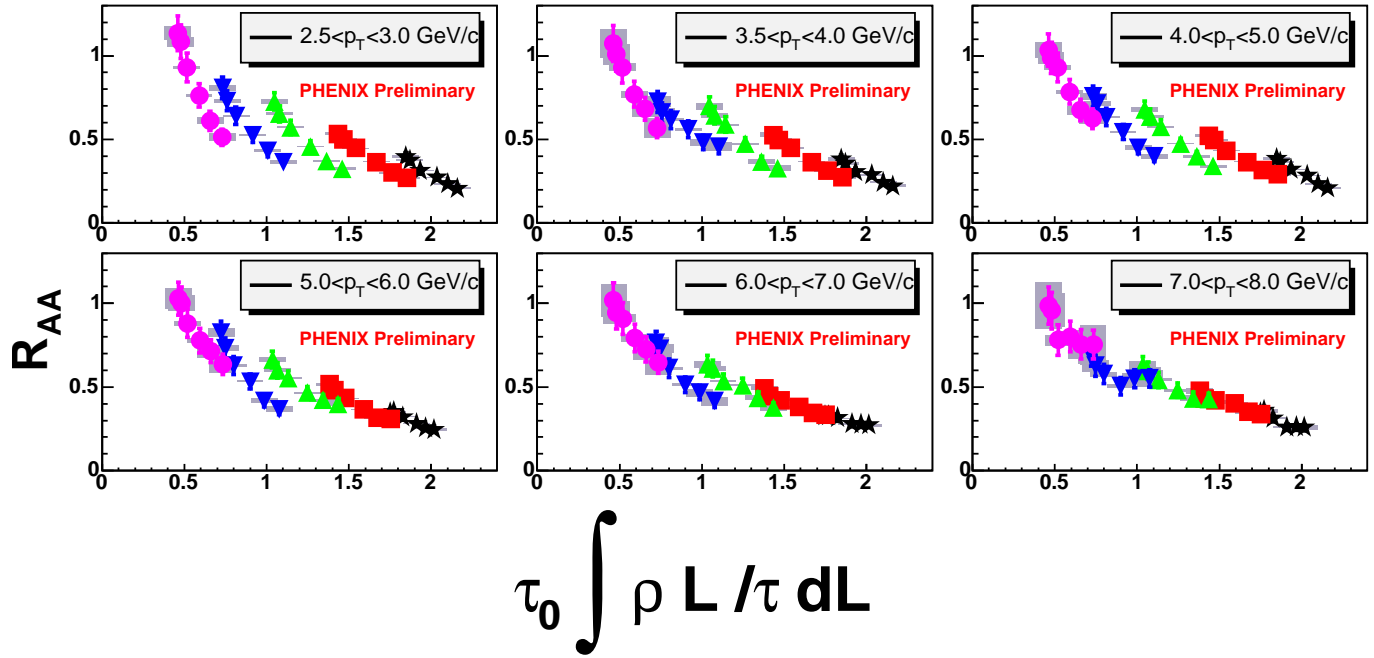


Fig. 5. $R_{AA}(\Delta\phi, p_T)$ vs. $\rho L dL$. The panels correspond to different p_T ranges. The solid circles are the most peripheral events, while the solid stars are the most central events.